Organometallics **2008,** *27,* 2421–2427

Rate and Mechanism of the Oxidative Addition of Aryl Halides to Palladium(0) Complexes Generated *in Situ* from a Pd(0)−Triolefinic Macrocyclic Complex and Phosphines

Anna Serra-Muns,[†,‡] Anny Jutand,*[,†] Marcial Moreno-Mañas,[‡,§] and Roser Pleixats*[,‡]

Département de Chimie, Ecole Normale Supérieure, CNRS, 24 Rue Lhomond,
F-75231-Paris Cedex 5, France, and Department of Chemistry, Universitat Autònoma de Barcelona,
Cerdanyola del Vallès, 08193-Barcelona, Spain

Received February 14, 2008

The rate and mechanism of the oxidative addition of aryl halides (PhI, PhBr) to Pd(0) complexes generated *in situ* upon addition of phosphines (PPh_3, P*n*Bu_3, dppf) to the macrocyclic triolefinic complex Pd^0(**1a**) have been investigated in THF or DMF. The macrocyclic ligand **1a** is known to allow a good recycling of the catalyst in catalytic reactions. It is established that the ligand **1a** affects the kinetics of oxidative addition, as monitored by electrochemical techniques. As far as PPh_3 is concerned, a reactivity order with PhI has been established in THF, $Pd^0(PPh_3)_4$ > {Pd^0(**1a**) + 4 PPh_3}, as a consequence of an equilibrium between Pd^0(**1a**) and $Pd^0(PPh_3)_3$ which decreases the concentration of $Pd^0(PPh_3)_3$ and consequently that of the reactive $Pd^0(PPh_3)_2$. As expected, {Pd^0(**1a**) + 2 PPh_3} is more reactive than {Pd^0(**1a**) + 4 PPh_3}. In contrast to PPh_3, the addition of *n* equivalents of P*n*Bu_3 to Pd^0(**1a**) in DMF leads to the formation of $Pd^0(\eta^2$-**1a**)(P*n*$Bu_3)_2$ and Pd^0(P*n*$Bu_3)_3$ (*n* > 2), characterized by ^{31}P NMR. At equal phosphine/Pd loading, the Pd(0) complex ligated by P*n*Bu_3 is more reactive than that ligated by PPh_3 and allows activation of PhBr at 25 °C in DMF. When *n* = 2, Pd^0(P*n*$Bu_3)_2$ is the unique species, which reacts with PhBr, but its concentration is controlled by the concentration of **1a**, which favors the formation of the unreactive $Pd^0(\eta^2$-**1a**)(P*n*$Bu_3)_2$ in a reversible reaction. The rate of the oxidative addition is limited by the dissociation of $Pd^0(\eta^2$-**1a**)(P*n*$Bu_3)_2$ to the reactive Pd^0(P*n*$Bu_3)_2$ at high PhBr concentrations (>0.04 M). The reaction with PhI involves both Pd^0(P*n*$Bu_3)_2$ and $Pd^0(\eta^2$-**1a**)(P*n*$Bu_3)_2$ as reactive species. The addition of 1 equiv of dppf to Pd^0(**1a**) leads to a complex mixture of Pd(0) complexes in THF. A reactivity order with PhI has been established, {Pd^0(**1a**) + 2 PPh_3} > {Pd^0(**1a**) + 1 dppf}, in THF at 25 °C.

Introduction

Some of us discovered[1] air- and moisture-stable phosphine-free macrocyclic triolefinic palladium(0) complexes of the type Pd^0(**1**) (Chart 1). The preparation[2,3] of the required 15-membered triolefinic azamacrocycles (**1**), their coordination properties[3,4] with transition metals, and the activity of Pd^0(**1**) as reusable catalysts[3,5] have been reported. Thus, complexes Pd^0(**1**) were active in Suzuki cross-couplings with activated aryl iodides.[5a] Polymeric versions (polystyrene-grafted catalyst[5a] and macrocycle-based polypyrrole-modified electrodes[5e]) were recovered and reused. Activated and deactivated aryl iodides gave good Suzuki couplings under catalysis by silica hybrids containing macrocyclic complexes covalently anchored.[5d,f,g] Although these results were promising, they have the limitation that only aromatic iodides showed activity in the Suzuki reaction. Very recently, the cross-coupling between arenediazonium salts and potassium organotrifluoroborates catalyzed by these macrocyclic complexes has been described.[5h] The macrocyclic complex catalyzed also the Mizoroki−Heck reactions with arenediazonium tetrafluoroborates as electrophilic partners[5c] and the hydroarylation of alkynes in ionic liquids,[5b] the complex being efficiently recovered in both cases.

On the other hand, complexes Pd^0(**1**) were not active in telomerization of butadiene in the presence of methanol. However, upon addition of phosphines, the reaction took place and the catalytic species could be recycled up to four times by adding fresh phosphine each time.[6] Subsequent mechanistic studies showed that Pd^0(**1**) complexes reacted with monodentate or bidentate phosphines to afford Pd^0L_n complexes.[7] After catalysis came to an end, if the phosphine was oxidized, palladium(0) reverted to the free macrocycle ligand, thus preventing agglomeration and precipitation as palladium black and remaining available for a new run, which required addition of fresh phosphine but not fresh palladium. With these precedents in mind we performed successful Suzuki cross-

---

* Corresponding authors. E-mail: Anny.Jutand@ens.fr; Roser.Pleixats@uab.cat.

[†] Ecole Normale Supérieure, CNRS.

[‡] Universitat Autònoma de Barcelona.

[§] Deceased on February 20, 2006.

(1) Cerezo, S.; Cortés, J.; López-Romero, J. M.; Moreno-Mañas, M.; Parella, T.; Pleixats, R.; Roglans, A. *Tetrahedron* **1998**, *54*, 14885.

(2) Cerezo, S.; Cortés, J.; Galvan, D.; Lago, E.; Marchi, C.; Molins, E.; Moreno-Mañas, M.; Pleixats, R.; Torrejón, J.; Vallribera, A. *Eur. J. Org. Chem.* **2001**, 329.

(3) For reviews on the synthesis and organometallic chemistry of 15-membered triolefinic macrocycles and the catalytic properties of their palladium(0) complexes, see: (a) Moreno-Mañas, M.; Pleixats, R.; Sebastián, R. M.; Vallribera, A.; Roglans, A. *Arkivoc (Part IV)* **2004**, 109, available from http://www.arkat-usa.org. (b) Moreno-Mañas, M.; Pleixats, R.; Sebastián, R. M.; Vallribera, A.; Roglans, A. *J. Organomet. Chem.* **2004**, *689*, 3669.

(4) Cerezo, S.; Cortés, J.; Lago, E.; Molins, E.; Moreno-Mañas, M.; Parella, T.; Pleixats, R.; Torrejón, J.; Vallribera, A. *Eur. J. Inorg. Chem.* **2001**, 1999.

10.1021/om800135n CCC: $40.75 © 2008 American Chemical Society
Publication on Web 05/09/2008

Chart 1

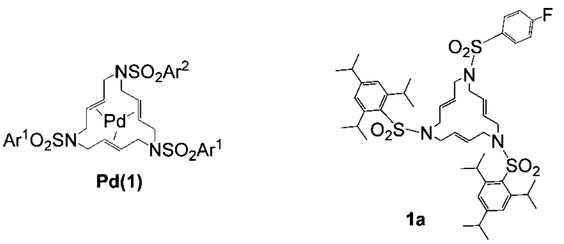

Pd(1)

1a

couplings on aryl and heteroaryl bromides and chlorides by using a catalytic system that was a combination of a bulky aliphatic σ-donor phosphine with a macrocyclic complex of type $Pd^0(\mathbf{1})$.[8] The addition of highly nucleophilic and sterically demanding phosphines allowed the activation of the more challenging bromides and chlorides,[9] and the macrocycle **1** allowed the recovery of the metal in the form of the initial macrocyclic complex.

The high dependence of the efficiency of catalytic reactions on phosphine structures prompted us to investigate the rate and mechanism of the first step of the catalytic cycles: the oxidative addition of aryl halides to the Pd(0) complexes generated *in situ* from $Pd^0(\mathbf{1a})$ (**1a**: *E*,*E*,*E*-1-(4-fluorophenylsulfonyl)-6,11-bis[(2,4,6-triisopropylphenyl)sulfonyl]-1,6,11-triazacyclopentadeca-3,8,13-triene) (Chart 1) associated with monophosphines (PPh_3, P*n*Bu$_3$) or a bisphosphine (dppf: 1,1′-bis(diphenylphosphino)ferrocene).

Rate and Mechanism of the Oxidative Addition of PhI to the Pd(0) Complex Generated *in Situ* from $Pd^0(1a)$ and *n* equiv of PPh_3 ($n \geq 2$). The cyclic voltammogram of $Pd^0(\mathbf{1a})$ (2 mM) in THF (containing $n\mathrm{Bu_4NBF_4}$, 0.3 M) did not exhibit any oxidation or reduction peak in the investigated potential range (+1.5 to −2.2 V vs SCE). After addition of 4 equiv of PPh_3, an oxidation peak was observed at $E^p{}_{O1} = +\ 0.45$ V vs SCE at 25 °C (Figure 1a). At least 1 h was required to observe a constant oxidation peak current, attesting to a slow reaction of $Pd^0(\mathbf{1a})$ with PPh_3. The cyclic voltammetry was similar to that of an authentic sample of $Pd^0(PPh_3)_4$ at the same concentration, which quantitatively generated $Pd^0(PPh_3)_3$ (oxidation peak at O_1, Figure 1b) as the major complex in THF, as previously reported,[10] except that the peak current was slightly higher in the latter case.

The oxidation peak current of $Pd^0(PPh_3)_3$ at O_1 was lower when 2 or 3 equiv of PPh_3 were added to $Pd^0(\mathbf{1a})$ (Figure S1 in the Supporting Information), suggesting that $Pd^0(PPh_3)_3$ was generated from $Pd^0(\mathbf{1a})$ in a reversible reaction (Scheme 1). Such equilibrium was also observed by ^{19}F NMR (235.36 MHz, CCl_3F) performed in THF on a solution of $Pd^0(\mathbf{1a})$ (0.01 M) after successive addition of PPh_3 (n = 3, 4, 5 equiv). Two multiplets were observed that characterized $Pd^0(\mathbf{1a})$ at −108.48 ppm and the free macrocyclic ligand **1a** at −108.65 ppm. Their relative magnitude varied with *n*, as in an equilibrium.

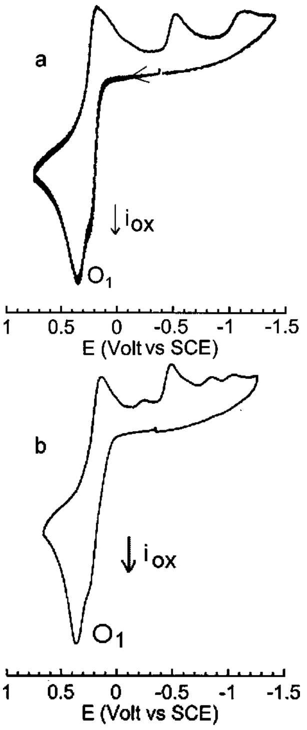

Figure 1. Cyclic voltammetry performed in THF (containing $n\mathrm{Bu_4NBF_4}$ 0.3 M) at a steady gold disk electrode (d = 0.5 mm) with a scan rate of 0.5 V s^{-1}, at 25 °C. (a) Oxidation of $Pd^0(PPh_3)_3$ generated *in situ* by addition of PPh_3 (8 mM) to $Pd^0(\mathbf{1a})$ (2 mM). (b) Oxidation of $Pd^0(PPh_3)_3$ generated *in situ* from $Pd^0(PPh_3)_4$ (2 mM). The current scale is the same on both voltammograms.

Scheme 1

$$Pd^0(\mathbf{1a}) + 3\ PPh_3 \xrightleftharpoons{K_0} Pd^0(PPh_3)_3 + \mathbf{1a}$$

No intermediate complexes such as $Pd^0(\eta^2\text{-}\mathbf{1a})(PPh_3)_2$ or $Pd^0(\eta^4\text{-}\mathbf{1a})(PPh_3)$ were detected on the ^{19}F NMR spectra, suggesting that the three C═C bonds of the macrocyclic ligand were substituted by 3 PPh_3. The ligand **1a** was quantitatively displaced from $Pd^0(\mathbf{1a})$ in the presence of 6 equiv of PPh_3. The equilibrium constant $K_0 = [PdL_3][\mathbf{1a}]/[Pd^0(\mathbf{1a})][L]^3$ was estimated from the ^{19}F NMR data (Scheme 1): $K_0 = 5.2 \times 10^3$ M^{-2} (THF, 25 °C) (Figure S2 in the Supporting Information).

The oxidation peak of $Pd^0(PPh_3)_3$ at O_1 generated upon addition of PPh_3 (4 equiv) to $Pd^0(\mathbf{1a})$ (2 mM) disappeared upon addition of excess iodobenzene, as a consequence of an oxidative addition that produced *trans*-$PhPdI(PPh_3)_2$ (characterized by ^{31}P and ^1H NMR by comparison to an authentic sample).[11] The kinetics of the oxidative addition was followed by chronoamperometry at a rotating gold disk electrode polarized at +0.5 V on the oxidation wave of $Pd^0(PPh_3)_3$.[10] The decrease of the oxidation plateau current of $Pd^0(PPh_3)_3$ (proportional to its

---

(5) (a) Cortés, J.; Moreno-Mañas, M.; Pleixats, R. *Eur. J. Org. Chem.* **2000**, 239. (b) Cacchi, S.; Fabrizi, G.; Goggiamani, A.; Moreno-Mañas, M.; Vallribera, A. *Tetrahedron Lett.* **2002**, *43*, 5537. (c) Masllorens, J.; Moreno-Mañas, M.; Pla-Quintana, A.; Roglans, A. *Org. Lett.* **2003**, *5*, 1559. (d) Blanco, B.; Mehdi, A.; Moreno-Mañas, M.; Pleixats, R.; Reyé, C. *Tetrahedron Lett.* **2004**, *45*, 8789. (e) Llobet, A.; Masllorens, E.; Rodriguez, M.; Roglans, A.; Benet.Buchholz, J. *Eur. J. Inorg. Chem.* **2004**, 1601. (f) Blanco, B.; Brissart, M.; Moreno-Mañas, M.; Pleixats, R.; Mehdi, A.; Reyé, C.; Bouquillon, S.; Hénin, F.; Muzart, J. *Appl. Catal. A Gen.* **2006**, *297*, 117. (g) Blanco, B.; Moreno-Mañas, M.; Pleixats, R.; Mehdi, A.; Reyé, C. *J. Mol. Catal. A: Chem.* **2007**, *269*, 204. (h) Masllorens, J.; Gonzalez, I.; Roglans, A. *Eur. J. Org. Chem.* **2007**, 158.

(6) Estrine, B.; Blanco, B.; Bouquillon, S.; Hénin, F.; Moreno-Mañas, M.; Muzart, J.; Pena, C.; Pleixats, R. *Tetrahedron Lett.* **2001**, *42*, 7055.

(7) Moreno-Mañas, M.; Pleixats, R.; Spengler, J.; Chevrin, C.; Estrine, B.; Bouquillon, S.; Hénin, F.; Muzart, J.; Pla-Quintana, A.; Roglans, A. *Eur. J. Org. Chem.* **2003**, 274.

(8) Moreno-Mañas, M.; Pleixats, R.; Serra-Muns, A. *Synlett* **2006**, 3001.

(9) (a) Littke, A. F.; Fu, G. C. *Angew. Chem., Int. Ed.* **2002**, *41*, 4176. (b) Bedford, R. B.; Cazin, C. S. J.; Holder, D. *Coord. Chem. Rev.* **2004**, *248*, 2283. (c) Farina, V. *Adv. Synth. Catal.* **2004**, *346*, 1553.

(10) (a) Fauvarque, J. F.; Pflüger, F.; Troupel, M. *J. Organomet. Chem.* **1981**, *208*, 419–427. (b) Amatore, C.; Jutand, A.; Khalil, F.; M'Barki, M. A.; Mottier, L. *Organometallics* **1993**, *12*, 3168–3178.

(11) Fitton, P.; Johnson, M. P.; McKeon, J. E. *J. Chem. Soc., Chem. Commun.* **1968**, 6–8.

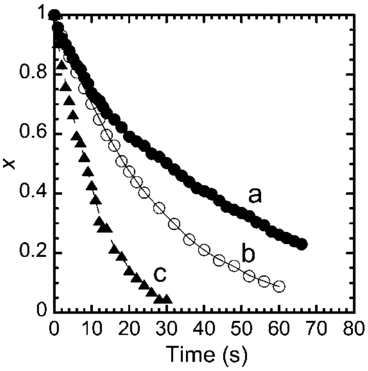

Figure 2. Kinetics of the oxidative addition of PhI (2 mM): (a) to the Pd(0) complex generated from $Pd^0(\mathbf{1a})$ (2 mM) and PPh_3 (8 mM); (b) to the Pd(0) complex generated from $Pd^0(PPh_3)_4$ (2 mM); (c) to the Pd(0) complex generated from $Pd^0(\mathbf{1a})$ (2 mM) and PPh_3 (4 mM) in THF (containing $n Bu_4NBF_4$ 0.3 M) at 25 °C. Plot of the molar fraction x of $Pd^0(PPh_3)_3$ against time ($x = [Pd(0)]/[Pd(0)]_0 = i/i_0$; i: oxidation plateau current of $Pd^0(PPh_3)_3$ in the presence of PhI at t, i_0: initial oxidation plateau current of $Pd^0(PPh_3)_3$, measured at a rotating gold disk electrode ($d = 2$ mm) polarized at +0.5 V vs SCE).

Table 1. Half-Reaction Times, $t_{1/2}$, of the Oxidative Addition of PhI (2 mM) or PhBr (2 mM) to Pd(0) Complexes Generated from Pd(0) Precursors (C_0 = 2 mM) at 25 °C

	$t_{1/2}$ (s)		
	PhI		PhBr
precursor	THF	DMF	DMF
$Pd^0(PPh_3)_4$	18		
$Pd^0(\mathbf{1a})$ + 4 PPh_3	30	17	
$Pd^0(\mathbf{1a})$ + 2 PPh_3	8		
$Pd^0(\mathbf{1a})$ + 2 $PnBu_3$		2.8	800
$Pd^0(\mathbf{1a})$ + 1 dppf	75		

Scheme 2

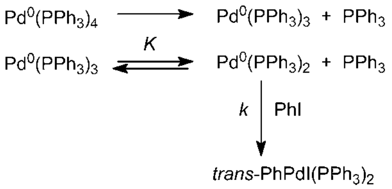

concentration) was recorded with time after addition of PhI (1 equiv, 2 mM). The half-life of the reaction was determined (Figure 2a, Table 1).

The kinetics of the oxidative addition was compared to that of $Pd^0(PPh_3)_4$ (Figure 2b) and $Pd^0(\mathbf{1a})$ + 2 equiv of PPh_3 (Figure 2c) ([PhI] = [Pd(0) precursor] = 2 mM). The following reactivity order has been established in THF (Table 1):

$$\{Pd^0(\mathbf{1a}) + 2\,PPh_3\} > Pd^0(PPh_3)_4 > \{\,Pd^0(\mathbf{1a}) + 4\,PPh_3\} \qquad (1)$$

In all cases, the reactive species was $Pd^0(PPh_3)_2$, as previously established when the precursor is $Pd^0(PPh_3)_4$ (Scheme 2).[10]

The fact that the oxidative addition was slower when performed from $Pd^0(\mathbf{1a})$ + 4 equiv of PPh_3 than from $Pd^0(PPh_3)_4$ suggests that the concentration of the reactive $Pd^0(PPh_3)_2$ was lower in the former case due to equilibrium of $Pd^0(PPh_3)_3$ with $Pd^0(\mathbf{1a})$, which decreased the $Pd^0(PPh_3)_3$ concentration and that of $Pd^0(PPh_3)_2$ as well (Scheme 3). The initial oxidation plateau current of $Pd^0(PPh_3)_3$ generated from $Pd^0(PPh_3)_4$ (2 mM) measured at a rotating gold disk electrode at +0.5 V was i_0 = 93.4 μA, whereas i_0 = 82.8 μA for $Pd^0(PPh_3)_3$ generated from $Pd^0(\mathbf{1a})$ (2 mM) and PPh_3 (8 mM), evidencing that $Pd^0(PPh_3)_3$ was initially generated at higher concentration from the $Pd(PPh_3)_4$ precursor.

Scheme 3

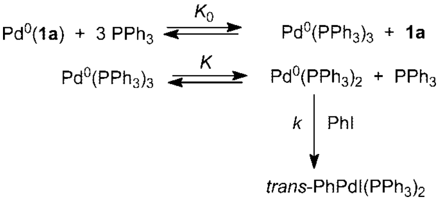

Scheme 4

$$[Pd(0)]_t = [Pd^0(\mathbf{1a})\,] + [PdL_3] + [PdL_2] = [PdL_2]\left(\frac{[\mathbf{1a}]}{K_0K[L]^2} + \frac{[L]}{K} + 1\right) \quad \text{with} \quad \frac{[L]}{K} >> 1$$

$$\frac{d[Pd(0)]_t}{dt} = -\frac{kK[PhI][Pd(0)]_t}{\dfrac{[\mathbf{1a}]}{K_0[L]^2} + [L]}$$

$$\frac{d[Pd(0)]_t}{[Pd(0)]_t} = -A[PhI]dt \quad \text{with } A = \frac{kK}{\dfrac{[\mathbf{1a}]}{K_0[L]^2} + [L]}$$

The kinetic law is expressed as rate = $k[PhI][PdL_2]$ (L = PPh_3).

Under stoichiometric conditions ($[Pd^0(\mathbf{1a})] = [PhI] = C_0$), the kinetic law becomes $1/x = 1 + AC_0t$ (see the expression of A in Scheme 4). The value of A was considered as constant in a first approximation.[12] The plot of $1/x$ was indeed linear (Figure 3a). The slope of the straight line delivers the value of A = 16.5 M^{-1} s^{-1} (THF, 25 °C). When the same reaction was performed from $Pd^0(\mathbf{1a})$ associated with 2 equiv of PPh_3, the oxidative addition of PhI was faster (Table 1). The plot of $1/x$ against time is shown in Figure 3b. The reaction obeyed the kinetic law $1/x = 1 + A'C_0t$ with A' = 54 M^{-1} s^{-1} (THF, 25 °C). A and A' are expressed by the same equation (Scheme 4) except that the phosphine concentration was lower in the latter case. This is why $A' > A$.

The oxidative addition was faster when performed in DMF (Table 1).[13]

Rate and Mechanism of the Oxidative Addition of PhX (X = I, Br) to the Pd(0) Complexes Generated *in Situ* from Pd^0(1a) and $PnBu_3$ (n equiv, $n \geq 2$). The reaction of $Pd^0(\mathbf{1a})$ with $PnBu_3$ (2 equiv) has been investigated in THF by cyclic voltammetry and ^{31}P NMR. Surprisingly, some Pd(II) complex was observed by cyclic voltammetry, leading to the conclusion that the Pd(0) complexes formed *in situ* were involved in some reaction with the solvent THF. The signals observed in ^{31}P NMR did not characterize a Pd(0) complex since they did not disappear after addition of PhI.

The reaction performed in DMF was more straightforward. The ^{31}P NMR spectrum of a solution of $Pd^0(\mathbf{1a})$ (7 mM) and $PnBu_3$ (14 mM) exhibited a minor broad signal centered at −32.30 ppm (<15%) and two doublets of similar magnitude at +16.09 ppm (J_{PP} = 40 Hz) and +18.80 ppm (J_{PP} = 40 Hz) (Figure S3 in the Supporting Information). After addition of PhI (1 equiv), a sharp singlet appeared at +3.09 ppm, which characterizes the complex *trans*-$PhPdI(PnBu_3)_2$ formed in the

---

(12) When n = 4 equiv of PPh_3, $[PPh_3]$ varied from $2.65C_0$ to $2C_0$. $[\mathbf{1a}]$ varied from $0.45C_0$ to C_0.

(13) The rotating disk electrode was polarized at +0.15 V vs SCE to avoid the oxidation of iodide anions, which were released in the oxidative addition due to the dissociation of $PhPdI(PPh_3)_2$ to $PhPd(DMF)(PPh_3)_2^+$.[14]

(14) Amatore, C.; Carré, E.; Jutand, A. *Acta Chem. Scand.* **1998**, *52*, 100–106.

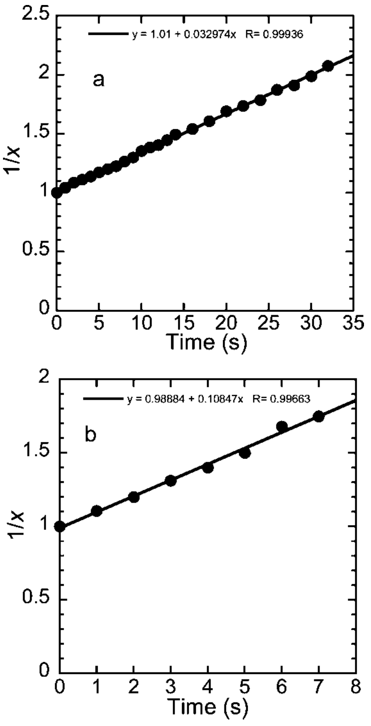

Figure 3. Kinetics of the oxidative addition of PhI (2 mM) to the Pd(0) complex generated from Pd^0(**1a**) (2 mM) and (a) PPh_3 (8 mM); (b) PPh_3 (4 mM) in THF (containing nBu_4NBF_4 0.3 M) at 25 °C. Plot of $1/x$ against time (x = molar fraction of $Pd^0(PPh_3)_3$; $x = [Pd(0)]_t/[Pd(0)]_0 = i/i_0$; i: oxidation plateau current of $Pd^0(PPh_3)_3$ in the presence of PhI at t, i_0: initial oxidation plateau current of $Pd^0(PPh_3)_3$ measured at a rotating gold disk electrode (d = 2 mm) polarized at +0.5 V vs SCE).

Scheme 5

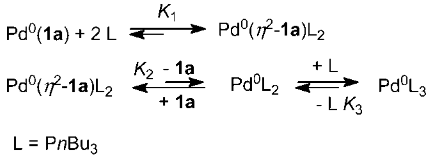

Scheme 6

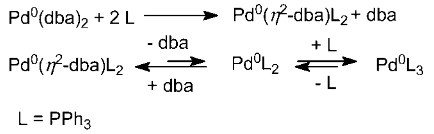

oxidative addition of a Pd(0) complex. The same singlet was indeed observed for *trans*-$PhPdI(PnBu_3)_2$ generated upon addition of excess $PnBu_3$ to *trans*-$PhPdI(PPh_3)_2$ in DMF.

When two more equivalents of $PnBu_3$ were added to the NMR tube containing Pd^0(**1a**) and 2 equiv of $PnBu_3$, the broad singlet at −32.33 ppm became thinner and its magnitude increased at the expense of that of the two doublets (Figure S4 in the Supporting Information). The effect was amplified after addition of two more equivalents of $PnBu_3$ (Figure S5 in the Supporting Information). The shift of the broad signal slightly differed from that of the free $PnBu_3$ (−32.44 ppm), which was never observed. One concludes that at low $PnBu_3$ loading ($PnBu_3/Pd^0$(**1a**) = 2) a main complex was formed that contained two non magnetically equivalent $PnBu_3$, leading to two ^{31}P NMR doublets. This attests to a complexation of $Pd^0(PnBu_3)_2$ to one C═C bond of the ligand **1a**, as in $Pd^0(\eta^2$-**1a**$)(PnBu_3)_2$ (a 16-electron complex). At higher $PnBu_3$ loading ($PnBu_3/Pd^0$(**1a**) = 4 or 6), $Pd^0(PnBu_3)_3$[15] was formed in equilibrium with $Pd^0(PnBu_3)_2$ and $PnBu_3$, at the expense of $Pd^0(\eta^2$-**1a**$)(PnBu_3)_2$ (Scheme 5). The higher stability of $Pd^0(\eta^2$-**1a**$)(PnBu_3)_2$ than that of $Pd^0(\eta^2$-**1a**$)(PPh_3)_2$ (never detected in ^{31}P NMR) may be rationalized by the fact that $Pd^0(PnBu_3)_2$, which is more electron rich than $Pd^0(PPh_3)_2$, easily coordinates one C═C bond of the ligand **1a** to decrease its electron density.

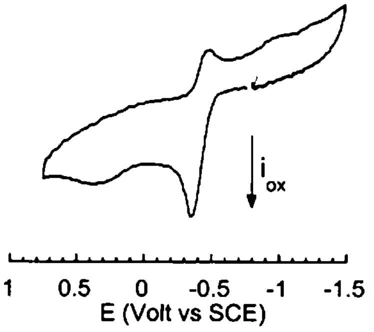

Figure 4. Cyclic voltammetry at a steady gold disk electrode (d = 0.5 mm) with a scan rate of 0.5 V s^{-1} of a solution of Pd^0(**1a**) (2 mM) and $PnBu_3$ (4 mM) in DMF (containing nBu_4NBF_4 0.3 M) at 25 °C.

Such a mechanism is very reminiscent of that for the formation of Pd(0) complexes upon addition of excess PPh_3 to $Pd^0(dba)_2$ (Scheme 6),[10b,16] except that the reaction of Pd^0(**1a**) and 2 $PnBu_3$ is probably an equilibrium (see K_1 in Scheme 5), which allowed part of the ligand to generate some $Pd(PnBu_3)_3$ observed as a minor compound on the ^{31}P NMR spectrum of a solution of Pd^0(**1a**) and 2 $PnBu_3$.

The Pd(0) complexes formed upon addition of $PnBu_3$ (2 equiv) to Pd^0(**1a**) (2 mM) in DMF were characterized by cyclic voltammetry. Two oxidation peaks were detected at E^p_{ox} = +0.31 V assigned to $Pd^0(\eta^2$-**1a**$)(PnBu_3)_2$ and E^p_{ox} = −0.37 V vs SCE assigned to $Pd^0(PnBu_3)_2$[17,18] (Figure 4, Scheme 5).

The kinetics of the oxidative addition of PhI (2 mM) to the Pd(0) complexes generated from **1a** (2 mM) and $PnBu_3$ (4 mM) in DMF was followed by chronoamperometry at a rotating gold disk electrode polarized at −0.1 V. The reaction was faster than that performed from Pd^0(**1a**) (2 mM) and PPh_3 (4 mM) in THF (Table 1, Figure 7a). The plot of $1/x$ was linear (Figure 5).

Three kinds of mechanisms might be involved: (i) $Pd^0(\eta^2$-**1a**$)(PnBu_3)_2$ as the reactive species, (ii) $Pd^0(PnBu_3)_2$ as the reactive species, or (iii) both species reacting in parallel. The three mechanisms could be discriminated by the determination of the reaction order for the aryl halide. Since the reaction with PhI was very fast under stoichiometric conditions (Table 1, Figure 5), the kinetics of the oxidative addition of PhBr to the Pd(0) complexes generated from Pd^0(**1a**) (2 mM) and 2 $PnBu_3$ was investigated (Figure S6 in the Supporting Information). As expected, the oxidative addition of PhBr (2 mM) was slower

---

(15) Mann, B. E.; Musco, A. *J. Chem. Soc., Dalton Trans.* **1975**, 1673–1677.

(16) Amatore, C.; Jutand, A. *Coord. Chem. Rev.* **1998**, *178−180*, 511–528.

(17) The complex $Pd^0(PnBu_3)_2$ has been generated in the electrochemical reduction of $Pd^{II}Cl_2(PnBu_3)_2$ in DMF and characterized by an oxidation peak potential at−0.40 V vs SCE. See: Amatore, C.; Aziz, S.; Jutand, A.; Meyer, G.; Cocolios, P. *New J. Chem.* **1995**, *19*, 1047–1059.

(18) According to the ^{31}P NMR some $Pd^0(PnBu_3)_3$ must also be formed in a fast equilibrium with $Pd^0(PnBu_3)_2$, leading to a unique oxidation peak at−0.37 V vs SCE, whose current peak was not proportional to the thermodynamic concentration of the Pd(0) species but to a dynamic concentration due to a shift of the equilibrium with $Pd^0(\eta^2$-**1a**$)PnBu_3)_2$ toward their formation, as a consequence of their consumption in the diffusion layer by their oxidation at the steady electrode (CE mechanism).[16]

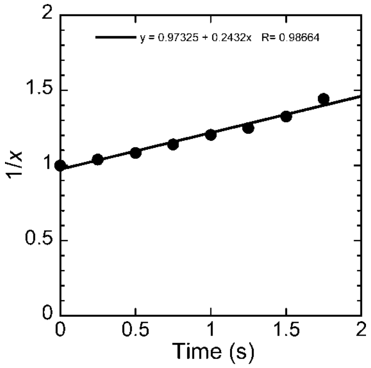

Figure 5. Kinetics of the oxidative addition of PhI (2 mM) to the Pd(0) complex generated from $Pd^0(\mathbf{1a})$ (2 mM) and $PnBu_3$ (4 mM) in DMF (containing nBu_4NBF_4 0.3 M) at 25 °C. Plot of $1/x$ against time ($x = [Pd^0(PnBu_3)_2]_t/[Pd^0(PnBu_3)_2]_0 = i/i_0$; i: oxidation plateau current of $Pd^0(PnBu_3)_2$ in the presence of PhI at t, i_0: initial oxidation plateau current of $Pd^0(PnBu_3)_2$ measured at a rotating gold disk electrode ($d = 2$ mm) polarized at −0.1 V vs SCE).

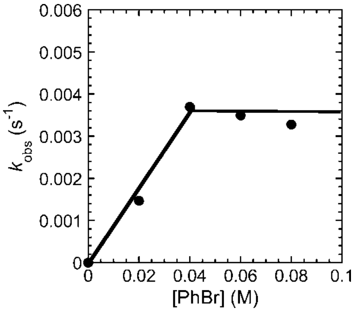

Figure 6. Kinetics of the oxidative addition of PhBr to the Pd(0) complex generated from $Pd^0(\mathbf{1a})$ (2 mM) and $PnBu_3$ (4 mM) in DMF (containing nBu_4NBF_4 0.3 M) at 25 °C.

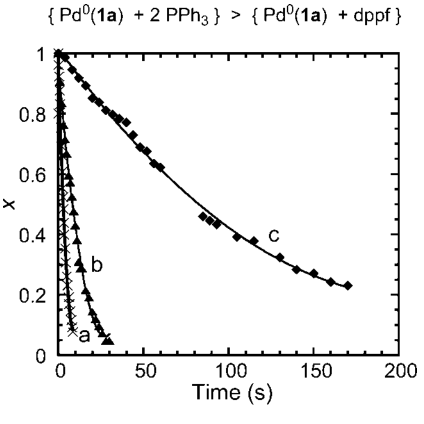

Figure 7. Kinetics of the oxidative addition of PhI (2 mM) to the Pd(0) complex generated from $Pd^0(\mathbf{1a})$ (2 mM) and (a) $PnBu_3$ (4 mM) in DMF; (b) PPh_3 (4 mM) in THF; (c) dppf (2 mM) in THF at 25 °C. Plot of the Pd(0) molar fraction x against time.

than that of PhI (2 mM) (Table 1). The reaction order for PhBr was determined by plotting ln x against time for different PhBr concentrations in the range 0.01−0.08 M: ln $x = -k_{obs}t$ (Figures S7−S10 in the Supporting Information). The plot of k_{obs} against PhBr concentration was linear at low PhBr concentrations (<0.04 M), attesting to a first-order reaction for PhBr (Figure 6). At higher PhBr concentrations, the reaction rate did not depend significantly on the PhBr concentration, attesting to a zero-order reaction for PhBr (Figure 6).

Scheme 7

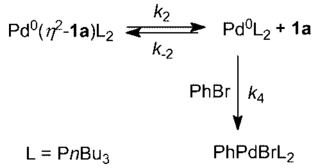

Scheme 8

$$\frac{d[Pd^0(\eta^2\text{-}\mathbf{1a})L_2]}{dt} = -\frac{k_4k_2[PhBr][Pd^0(\eta^2\text{-}\mathbf{1a})L_2]}{k_{-2}[\mathbf{1a}] + k_4[PhBr]}$$

$$\ln x = -\frac{k_4k_2[PhBr]}{k_{-2}[\mathbf{1a}] + k_4[PhBr]}\, t = -k_{obs}t$$

At low [PhBr] concentrations, $k_{-2}[\mathbf{1a}] > k_4[PhBr]$

$$k_{obs} = \frac{k_4K_2[PhBr]}{[\mathbf{1a}]}$$

At high [PhBr] concentrations, $k_{-2}[\mathbf{1a}] < k_4[PhBr]$

$$k_{obs} = k_2$$

Such behavior indicates that only one species is reactive and generated in a dissociation step as $Pd^0(PnBu_3)_2$ (Scheme 7). Since at low $PnBu_3$ loading ($PnBu_3$/Pd = 2) $Pd^0(PnBu_3)_3$ was formed as a minor complex, the contribution of the equilibrium between $Pd^0(PnBu_3)_3$ and $Pd^0(PnBu_3)_2$ (K_3 in Scheme 5) was neglected.

At high PhBr concentrations, the reaction rate did not depend on PhBr concentration because the reactivity of $Pd^0(PnBu_3)_2$ was limited by its rate of formation by dissociation of $Pd^0(\eta^2\text{-}\mathbf{1a})(PnBu_3)_2$ (rate constant k_2 in Scheme 7), in agreement with the kinetic law given in Scheme 8. The value of $k_2 = 0.0036$ s^{-1} (DMF, 25 °C) was determined from the limit in Figure 6. This indicates that whatever the aryl halide, the half-reaction time of the oxidative addition cannot be lower than $t_{1/2} = 190$ s, which is the half-reaction time of the dissociation of $Pd^0(PnBu_3)_2$ from $Pd^0(\eta^2\text{-}\mathbf{1a})(PnBu_3)_2$ (2 mM). Since the half-reaction time of the reaction of PhI (2 mM) with the Pd(0) generated from $Pd^0(\mathbf{1a})$ (2 mM) and $P(nBu_3)_2$ (4 mM) was found to be $t_{1/2} =$ 2.8 s (Table 1), this indicates that the oxidative addition of PhI also proceeds from $Pd^0(\eta^2\text{-}\mathbf{1a})(PnBu_3)_2$, which reacts in parallel with $Pd^0(PnBu_3)_2$. This mechanism might have been confirmed by the investigation of the reaction order for PhI.[19] Unfortunately, the very fast oxidative addition of PhI even under stoichiometric conditions prevented any accurate kinetic studies.

Rate of the Oxidative Addition of PhI to the Pd(0) Complexes Generated *in Situ* from Pd^0(1a) and dppf (1 equiv). The cyclic voltammogram of the Pd(0) complex(es) generated from $Pd^0(\mathbf{1a})$ (2 mM) in THF (containing nBu_4NBF_4, 0.3 M) and 1 equiv of the bidentate ligand dppf exhibited after 10 min two close oxidation peaks at +0.17 (major) and +0.29 vs SCE at 25 °C (Figure S10 in the Supporting Information). The peak currents did not change with time, attesting to a fast reaction of $Pd^0(\mathbf{1a})$ with dppf. The ^{31}P NMR spectrum of this mixture was quite complex. At least four sets of signals were detected. Among them two doublets were observed at +16.5 ppm ($J_{PP} = 96$ Hz) and +15.42 ppm ($J_{PP} = 96$ Hz). The high J_{PP} constant suggested a complex containing two different phosphorus in a *trans* position. Since the ^{31}P NMR was concentration dependent, the formation of dimeric complexes

---

[19] For a related mechanism involving the parallel reactivity of Pd^0(P,P) and $Pd^0(\eta^2\text{-dba})$(P,P) (P,P: bidentate phosphine ligand) with PhI, see ref 20.

where the Pd(0) moieties are still ligated to one C═C bond of **1a** and to one P of dppf, which behaved as a monodentate ligand, is not excluded. Upon addition of PhI (1 equiv), the signals disappeared, leading to two new doublets at 25.53 ppm (d, J_{PP} = 34 Hz, 1P) and +7.50 ppm (d, J_{PP} = 34 Hz, 1P), which characterized the complex PhPdI(dppf) formed in oxidative additions.[20] Consequently, a mixture of undefined Pd(0) ligated by dppf and by **1a** was formed and reacted with PhI. Even in the absence of clear structural data for these Pd(0) complexes, the reaction of PhI (2 mM) with the Pd(0) complexes generated *in situ* from Pd^0(**1a**) (2 mM) and dppf (2 mM) in THF was monitored by chronoamperometry performed at a rotating electrode polarized at +0.45 V (Figure 7c). From the half-reaction time of the reaction, it emerges that the oxidative addition of PhI is slower than that involving PPh_3 as ligand in THF (Figure 7b,c; Table 1, Figure S12).

Conclusion

Besides its ability to recover and recycle Pd(0) catalysts in catalytic reactions, the macrocyclic ligand **1a** plays an important role in the kinetics of the oxidative addition of aryl halides performed from Pd^0(**1a**) associated with phosphine ligands (PPh_3, P*n*Bu_3, dppf) in THF or DMF. The following reactivity order with PhI has been established:

$$\underset{\text{DMF}}{\mathrm{Pd^0}(\mathbf{1a}) + 2\,\mathrm{P}n\mathrm{Bu_3}} > \underset{\text{THF}}{\mathrm{Pd^0}(\mathbf{1a}) + 2\,\mathrm{PPh_3}} > \underset{\text{THF}}{\mathrm{Pd^0(PPh_3)_4}} > \underset{\text{THF}}{\mathrm{Pd^0}(\mathbf{1a}) + 4\,\mathrm{PPh_3}} > \underset{\text{THF}}{\mathrm{Pd^0}(\mathbf{1a}) + \mathrm{dppf}} \quad (2)$$

The ligand **1a** is in equilibrium with the reactive $Pd^0(PPh_3)_2$ complex via $Pd^0(PPh_3)_3$. The concentration and reactivity of $Pd^0(PPh_3)_2$ is controlled by the concentration of **1a**, and the oxidative addition of PhI is slower than that performed from **1a**-free precursors at equal ligand loading and Pd concentration (e.g., {Pd^0(**1a**) + 4 PPh_3} less reactive than $Pd^0(PPh_3)_4$). In contrast to PPh_3, **1a** is also a ligand in $Pd^0(\eta^2$-**1a**)(P*n*$Bu_3)_2$ which is in equilibrium with the most reactive Pd^0(P*n*$Bu_3)_2$ complex. Once more, the ligand **1a** plays an important role since the rate of the oxidative addition of PhBr is found to be limited by the dissociation of Pd^0(P*n*$Bu_3)_2$ from $Pd^0(\eta^2$-**1a**)(P*n*$Bu_3)_2$ at high PhBr concentrations. The reaction of PhI also involves $Pd^0(\eta^2$-**1a**)(P*n*$Bu_3)_2$ as the reactive species. The decelerating effect induced by the ligand **1a** can be of interest if the fast oxidative addition has to be slowed down so that its rate becomes closer to the rate of the following slower step (e.g., transmetalation or carbopalladation). This emphasizes the key role played by unsaturated C═C ligands of Pd(0) precursors in oxidative addition, as reported by some of us in the case of dba[16,21] or with extra olefins.[22]

Experimental Part

^{31}P NMR spectra were recorded on a Bruker spectrometer (101 MHz) with H_3PO_4 as an external reference. Cyclic voltammetry and chronoamperometry were performed at a gold disk electrode with a homemade potentiostat and a Tacussel GSTP4 waveform generator. The voltammograms were recorded on a Nicolet 301 oscilloscope. All experiments were performed under an argon atmosphere.

Chemicals. THF was distilled from Na/benzophenone. DMF was distilled from calcium hydride under vacuum and kept under argon. The ligands PPh_3, P*n*Bu_3, and dppf were commercial. The ligand **1a** was synthesized as indicated in the Supporting Information. $PhPdI(PPh_3)_2$ was prepared as described in the literature.[11]

Synthesis of Pd^0(1a). A 0.911 g (1.01 mmol) amount of the macrocycle **1a** and 1.52 g (1.32 mmol) of $Pd(PPh_3)_4$ in 50 mL of THF were stirred at reflux for 15 h. After filtration, the filtrate was evaporated under vacuum to give a residue that was purified through a silica gel column (hexane/ethyl acetate) to afford 720 mg of Pd(**1a**) as a white solid (71% yield). IR (ATR): ν 2955, 2867, 1593, 1311, 1148 cm^{-1}. ^{1}H NMR (250 MHz, TMS, $CDCl_3$): δ 1.28 (m, 36H), 1.77 (m, 2H), 2.12 (m, 3H), 2.91 (sept. J = 6.9 Hz, 2H), 3.21 (m, 3H), 3.85 (m, 2H), 4.17 (m, 6H), 4.64 (m, 6H), 7.18 (m, 6H), 7.81 (m, 2H) ppm. ^{19}F NMR (235.36 MHz, CCl_3F, $CDCl_3$): δ −108.48 (m, 1F). Anal. Calcd for $C_{48}H_{68}FN_3O_6S_3Pd$: C, 57.38; H, 6.82; N, 4.18; S, 9.57. Found: C, 57.27; H, 6.84; N, 4.10 ; S, 9.30.

General Procedure for Cyclic Voltammetry. Experiments were carried out in a three-electrode thermostated cell (25 °C) connected to a Schlenk line. The reference was a saturated calomel electrode (Radiometer) separated from the solution by a bridge filled with 1.5 mL of THF containing *n*Bu_4NBF_4 (0.3 M). The counter electrode was a platinum wire of ca. 1 cm^2 apparent surface area. Fifteen milliliters of THF containing *n*Bu_4NBF_4 (0.3 M) was introduced into the cell followed by 15.9 mg (0.06 mmol) of PPh_3 and 30.1 mg (0.03 mmol) of Pd^0(**1a**). Cyclic voltammetry was performed with time at a steady gold disk electrode (d = 0.5 mm) at a scan rate of 0.5 V s^{-1}. Increasing amounts of PPh_3 were then added to the cell, and cyclic voltammetry was performed with time at a scan rate of 0.5 V s^{-1}. Similar experiments were performed from 30.1 mg (0.03 mmol) of Pd^0(**1a**) in the presence of 16.8 mg (0.03 mmol) of dppf in THF or 15.7 μL (0.06 mmol) of P*n*Bu_3 in DMF.

General Procedure for the Kinetics of the Oxidative Addition of PhI to Pd(0) Complexes Generated *in Situ* from Pd^0(1a) Associated with PPh_3 or dppf. Experiments were carried out in the same cell as used for cyclic voltammetry (see above). Fifteen milliliters of THF containing *n*Bu_4NBF_4 (0.3 M) was introduced into the cell followed by 15.9 mg (0.06 mmol) of PPh_3 and 30.1 mg (0.03 mmol) of Pd^0(**1a**). After 1 h, the kinetic measurement for the oxidative addition of PhI was performed at a rotating gold disk electrode (Radiometer, EDI 65109, d = 2 mm, angular velocity ω = 105 rad s^{-1}) polarized at +0.5 V vs SCE. The decrease of the oxidation current of the Pd(0) complex was recorded with time after addition of 3.4 μL (0.03 mmol) of PhI until total conversion. Similar experiments were done in the presence of 32 mg (0.12 mmol) of PPh_3 or 16.8 mg (0.03 mmol) of dppf.

General Procedure for the Kinetics of the Oxidative Addition of PhBr to Pd(0) Complexes Generated *in Situ* from Pd^0(1a) Associated with P*n*Bu_3. The kinetics of the oxidative addition of PhBr (2, 20, 40, 60, and 80 mM) to the Pd(0) complex generated from 30.1 mg (0.03 mmol) of Pd^0(**1a**) and 15.7 μL (0.06 mmol) of P*n*Bu_3 in DMF was monitored at a rotating gold disk electrode as explained above in THF (see kinetic curves in the Supporting Information).

General Procedure for ^{31}P NMR (101.3 MHz, H_3PO_4) Experiments. To an NMR tube containing 0.5 mL of DMF and 0.1 mL of acetone-d_6 were added 9 mg (0.009 mmol) of Pd^0(**1a**) followed by 4.7 μL (0.018 mmol) of P*n*Bu_3. The ^{31}P NMR was performed from time to time. Similar experiments were performed

---

[20] Amatore, C.; Broeker, G.; Jutand, A.; Khalil, F. *J. Am. Chem. Soc.* **1997**, *119*, 5176–5185.

[21] (a) Fairlamb, I. J. S.; Kapdi, A. R.; Lee, A. F. *Org. Lett.* **2004**, *6*, 4435–4438. (b) Macé, Y.; Kapdi, A. R.; Fairlamb, I. J. S.; Jutand, A. *Organometallics* **2006**, *25*, 1795–1800. (c) Fairlamb, I. J. S.; Kapdi, A. R.; Lee, A. F.; McGlacken, G. P.; Weissburger, F.; de Vries, A. H. M.; Schmieder-van de Vondervoort, L. *Chem.−Eur. J.* **2006**, *12*, 8750–8761. (d) Fairlamb, I. J. S.; Lee, A. F. *Organometallics* **2007**, *26*, 4087–4089.

[22] For reviews on the effect of olefins on oxidative additions, see: (a) Jutand, A. *Pure Appl. Chem.* **2004**, *76*, 565–576. (b) Johnson, J. B.; Rovis, T. *Angew. Chem., Int. Ed.* **2008**, *47*, 840–871.

in the presence of increasing amounts of P*n*Bu$_3$: 4 and 6 equiv (see spectrum in the Supporting Information).

Similar experiments were performed from 9 mg (0.009 mmol) of Pd^0(**1a**) and 5 mg (0.009 mmol) of dppf in 0.5 mL of THF and 0.1 mL of acetone-d_6.

Acknowledgment. Financial support from MEC of Spain (Projects CTQ2005-04968-C02-01, CTQ2006-04204/BQU), Consolider Ingenio 2010 (Project CSD2007-00006), and Generalitat de Catalunya (Project SGR2005-00305) is gratefully acknowledged, as well as financial support from CNRS (UMR 8640) and Ecole Normale Supérieure (France).

Supporting Information Available: Graphs for the determination of equilibrium and rate constants and ^{31}P NMR spectra. These materials are available free of charge via the Internet at http://pubs.acs.org.

OM800135N